Article ID: 1006-8775(2011) 03-0310-07

EVOLUTION OF MOIST POTENTIAL VORTICITY DURING A WARM-ZONE HEAVY RAINFALL EVENT IN THE PEARL RIVER DELTA

LI Jiang-nan (李江南)[1], YE Ai-fen (叶爱芬)[1, 2], XU Yong-hui (徐永辉)[3], WU Zhi-fang (伍志方)[2], HE Ru-yi (何如意)[2], CAI Rong-shuo (蔡榕硕)[4]

(1. School of Environmental Science and Engineer, Sun Yat-sen University, Guangzhou 510275 China; 2. Guangzhou Meteorological Observatory, Guangzhou 510080 China; 3. Huadu District Bureau of Meteorology, Guangzhou 510800 China; 4. Key Laboratory of Global Change and Marine-Atmospheric Chemistry, Third Institute of Oceanography, State Oceanic Administration of China, Xiamen 361005 China)

Abstract: First, based on routine meteorological data, the synoptic characteristics of a heavy warm-sector rainfall that occurred on June 13, 2008 in the Pearl River Delta were analyzed. Second, a mesoscale numerical model, Weather Research and Forecasting (WRFV2.2), was used to simulate the heavy rainfall. Diagnostic analyses were done of moist potential vorticity (MPV) for its horizontal components (MPV2) and vertical components (MPV1) based on the simulation results of WRFV2.2 to identify the mechanism of the rainfall development. The results showed that the heavy rainfall occurred when there were high MPV1 in the upper levels and low MPV1 and high MPV2 in the lower levels. Disturbances of high MPV1 in the upper levels came from the southwest or northwest, those of low MPV1 in the lower levels came from the southwest, and those of high MPV2 came from the south. Disturbances of low MPV1 at low levels were the direct cause of convective instability. Enhanced vertical shear of meridional wind led to increased MPV2 at lower levels, strengthened baroclinicity, and active warm and wet flows. These distributions of MPV helped to trigger the release of unstable energy and produce warm-sector heavy rainfall. As it integrates the evolution of dynamic and thermal fields, MPV is able to reveal the development of this heavy rainfall effectively.

Key words: heavy rainfall; MPV(moist potential vorticity); numerical simulation

CLC number: P458.1.21 **Document code:** A **doi:** 10.3969/j.issn.1006-8775.2011.03.013

1 INTRODUCTION

Being a physical quantity that integrates both the dynamics and thermodynamics of the atmosphere, moist potential vorticity (MPV) is widely used in the research on heavy rain, typhoons and climate[1-3]. In his special study on the application of MPV in the heavy rain resulting from Mei-yu fronts in 1995, Wu[4] pointed out that the movement of large, positive MPV2 at the lower troposphere can be used as a tracer for the activity of low-level jet streams and warm and humid airflows or vortexes, and precipitation is likely to occur when negative MPV1 superimposes with positive MPV2 in the lower troposphere. With MPV, diagnostic analysis is conducted of heavy rains on Mei-yu fronts and unusually heavy rains in the northwest of China (Zhang et al.[5]; Wang et al.[6]; and Ren et al.[7]). When MPV1<0 and MPV2>0 at 700 hPa, severe precipitation will appear, as indicated in a diagnosis of an intense summertime rainfall in Yunnan (Fan and Ju[8]). In 2004, Meng et al.[9] pointed out that positive MPV anomalies mainly occur below the level of 700 hPa during hard rains, as shown in their diagnosis of a heavy rain in the south of China during May 23–24, 1998. The same heavy rain was diagnostically studied by Wen et a.[10], who found that the area of precipitation is below negative MPV.

In their study on a heavy rain taking place in the warm sector ahead of a front in the south of China in 2005, Xia et al.[11] concluded that one of the characteristics of this type of rain is its intense wind-speed convergence by low-level southerly airflows and frequent impacts of the rain core by low-level wind-speed convergence centers, which

Received 2010-09-28; **Revised** 2011-06-03; **Accepted** 2011-07-15

Foundation item: Open Foundation of the Key Laboratory on Ocean-Atmospheric Chemistry and Global Change from State Oceanological Administration (GCMAC0809); Natural Science Foundation of China (40775068); Development Planning for Key Foundamental Research of China (2010CB428504)

Biography: LI Jiang-nan, Ph.D., primarily undertaking research on heavy rain and typhoons affecting the south of China.

Corresponding author: LI Jiang-nan, e-mail: essljn@mail.sysu.edu.cn

cumulate and then release energy repeatedly while mesoscale convective cloud clusters affect the rain core for a number of times. For a severe warm-sector rainfall that took place in the Pearl River Delta on June 13, 2008, this work, having analyzed its synoptic background, used the Weather Research and Forecasting (WRF) model from the U.S.A. for numerical simulation. Based on its successful simulations, we applied the model-output high-resolution data for diagnostic study on the evolutions of MPV of this severe warm-sector rain.

2 DATA AND DESIGN OF MODEL SCHEME

The data employed here in this work include 1° ×1° gridpoint data from the National Centers for Environmental Protection (NCEP, USA) Final Analysis (FNL), surface and ship data and sounding data. All of them cover the time from 1200 Beijing Standard Time (BST) June 11 to 1200 BST June 14, 2008.

The model, a mesoscale WRFV2.2—two-layer nested with a 30-km grid interval and 74×61 gridpoints in the coarse mesh and a 10-km grid interval and 112×97 gridpoints in the fine mesh, is used. The WSM5-class scheme is used for the microphysics, Kain-Fritsch scheme (shallow convection) for parameterization of cumulus convection, RRTM scheme for longwave radiation, Dudhia scheme for shortwave radiation, Monin-Obukhov scheme for near-surface layers, YSU scheme for the boundary layer, and the thermal diffusion scheme for land processes, respectively. The integration adopts a time step of 180 seconds. The model updates the boundary condition once every six hours, and the outputs are available every three hours for the coarse mesh and every one hour for the fine mesh.

3 OBSERVATIONS OF THE INTENSE RAINFALL AND ITS SYNOPTIC BACKGROUND

3.1 *Observations of the intense rainfall*

During the first and second ten-day periods of June, 2008, processes of persistent, intense rain occurred across Guangdong, with the peak of rainfall appearing on June 13. From 2000 BST June 12 to 2000 BST June 13, exceptionally heavy rainfall was recorded at 56, unusually heavy rain at 309, and heavy rain at 342, of the 1300 automatic weather stations (AWSs) across the province. From 2000 BST June 13 to 2000 BST June 14, 149 AWSs had heavy rain with 92 of them reaching the intensity of unusually heavy rain. On a chart showing the distribution of cumulated rainfall from 2000 BST June 12 to 2000 BST June 14, it is more than 150 mm in the delta and southeastern part of the province, with the core of 48-h rainfall—almost 500 mm, located at Huidong in the delta.

The variation of hourly rainfall amount that covers the period from 2000 BST June 12 to 2000 BST June 14 is studied of the three delta stations at Guangzhou, Dongguan and Huidong (figure omitted). The precipitation of Guangzhou can be divided into four sections of time: from the early hours of the morning to the time before midday on June 13, the evening of June 13, the morning of June 14 (with maximum hourly rainfall of 30.2 mm), and the evening of June 14. For Dongguan, the precipitation concentrated on June 13 with the amount being 67.5 mm at 0600 BST, 84.6 mm at 0700 BST, and 67.3 mm at 0800 BST, respectively. In Huidong, the precipitation peaked during 1000–2300 BST on June 13 with an hourly rainfall of 62.3 mm at 1700 BST on June 13. On June 13, the Pearl River Delta witnessed a persistent severe rain, whose center was right over the area.

3.2 *Synoptic background*

At 0800 BST June 12, a 200-hPa South Asia high was steadily dominant over the region of the Tibetan Plateau and there was a major trough to its east north of 30° N, exposing Guangdong to an area of divergence of an northerly airflow (figure omitted). At 0500 BST June 13, the trough extended south to reach the north of the province, contributing to a pattern of divergence over the delta where Qingyuan, at the northwest of the province, had southwest-by-west winds (16 m/s), while Hong Kong, at the estuary of the Pearl River, experienced northerly winds (20 m/s). At 2000 BST June 13, the trough, now in front of the South Asia high, dominated over Guangdong with both Qingyuan and Hong Kong in the control of westerly winds of 16 m/s and Shantou, at the eastern side, prevalent with westerly winds of 22 m/s, constituting to intense divergence. The trough was over the province by 2000 BST June 14 but wind speed decreased in the trough area, weakening the intensity of divergence. On June 13, a 500-hPa upper-level trough began to affect Guangdong from the west, making southwesterly airflows strong ahead of the trough. On June 14, the upper-level trough moved east to sea while weakening such that the province was subject to a weak anti-cyclonic circulation, which decreased the precipitation.

At 850 hPa (Fig. 1), a shear was seen north of the Nanling Mountains at 0800 BST June 12. As Guangdong was within a southwesterly jet stream south of it, humidity rose so that at 2000 BST T-T_d across the province was in the range of 1–3° C. At 0800 BST June 13, the 850-hPa shear was a little southward but Guangdong stayed to the south of the shear with southerly winds as high as 20 m/s at the

Pearl River estuary and still at 14 m/s in the north of the province. Therefore, a strong convergence of wind speed existed over the Pearl River Delta. On June 14, the shear was shifted to northwestern Guangdong with the southerly changed to southwesterly in the central and southern parts of the province. The speed of the southwesterly also decreased, with 10 m/s at Hong Kong and 12 m/s at Shantou, changing the convergence to divergence over the delta. It is then known that during the intense rain, the Pearl River Delta was situated in an area of wind-speed convergence of the southwesterly flow located south of the shear. This result is consistent with the conclusion of Xia et al.[11] that one of the characteristics of the warm-sector heavy rain in the south of China is the intense convergence of wind speed of the low-level southerly airflow.

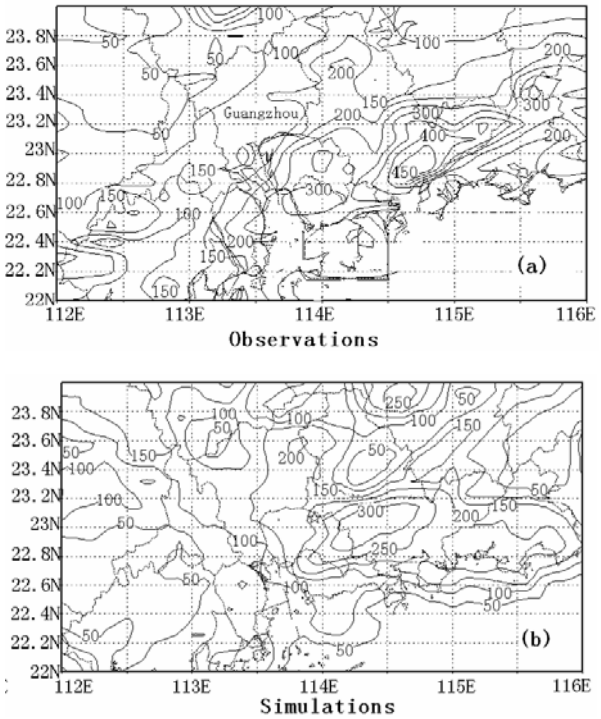

Fig. 1. Observations (a) and simulations (b) of the rainfall for 2000 BST June 12 to 2000 BST June 14, 2008. Unit: mm

On the surface level, the south of China was also affected by troughs. At 0800 BST June 13, a converging line occurred in southern Guangdong, which was in a trough area, with southerly winds to the south, and northerly winds to the north, of the converging line. The presence of strong wind-speed convergence at low levels is conducive to the accumulation of water vapor and energy.

4 COMPARISON OF SIMULATED RAINFALL TO OBSERVED RAINFALL

Examination of 48-h cumulated rainfall (Fig. 2) shows that the observed rainfall is consistent with the simulated rainfall in the distribution. They both center on Huizhou, which is located in the delta, with main rainbands positioned in an east-west direction. In particular, the rainfall for Guangzhou is very close between the observation and model output, which is between 50 mm and 150 mm. They distribute in similar patterns with more rain in the east than in the west. For the temporal variation of rainfall, the model output is also consistent with the observation (figure omitted). In general, the WRF model was successful in simulating this rainfall event, except for smaller maximum of the rainfall center. This finding is also similar to the result of Grams et al.[12] This precipitation of Guangzhou can be divided into three stages: Stage One started from the early hours of the morning of June 13 and ended at 1600 BST the same day, with a total rainfall of about 80 mm. Stage Two covered the early hours of the morning of June 14, with a total rainfall of about 30 mm. Stage Three lasted from 1400–2000 BST June 14, with a total rainfall of about 10 mm. In the following sections, the model output will be studied for MPV based on the above successful simulations, with the focus on Stage One.

5 EVOLUTIONS OF MPV ON ISOBARIC SURFACES

By ignoring the horizontal change of ω (vertical velocity), an expression for MPV can be approximately written as follows:

$$\mathrm{MPV}=-g(\zeta+f)\frac{\partial\theta_e}{\partial p}+g\left(\frac{\partial v}{\partial p}\frac{\partial\theta_e}{\partial x}-\frac{\partial u}{\partial p}\frac{\partial\theta_e}{\partial y}\right)$$

where ζ is the vertical component of absolute vorticity, θ_e the equivalent potential temperature, MPV>0 indicates that the atmosphere is stable with moist symmetric condition, and MPV<0 depicts that the atmosphere is unstable with moist symmetric condition. MPV = MPV1 + MPV2. MPV1 = $-g(\zeta+f)\frac{\partial\theta_e}{\partial p}$, which is the vertical component of MPV. Its value depends on the product of the vertical component of absolute vorticity multiplied by that of the equivalent potential temperature, called the term of moist, barotropic potential vorticity. When the atmosphere is convectively unstable, $\frac{\partial\theta_e}{\partial p}$ >0, MPV1<0. MPV2= $g\left(\frac{\partial v}{\partial p}\frac{\partial\theta_e}{\partial x}-\frac{\partial u}{\partial p}\frac{\partial\theta_e}{\partial y}\right)$. The value of the horizontal component of MPV depends on the vertical shear of the wind and the term of moist baroclinity. By studying the MPV2, the baraclinity of weather systems and the activity of warm and moist airflows can be recognized.

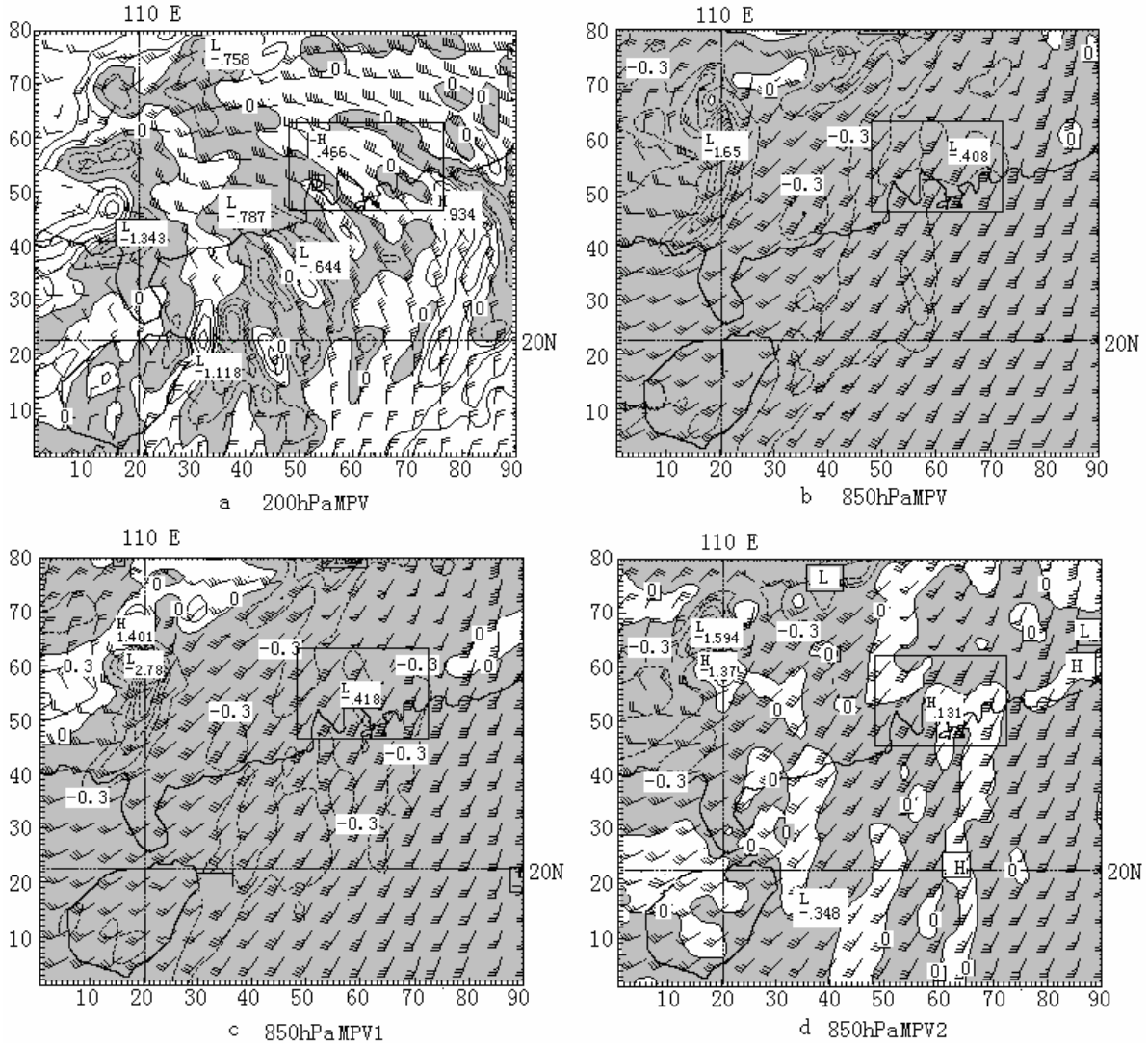

Fig. 2. Model-output 200-hPa MPV (a), 850-hPa MPV (b), MPV1 (c), and MPV2 (d) for 1000 BST June 13, 2008. Grey areas indicate negative values and white areas stand for positive values. 1 PVU=10^{-6} m^2 s^{-1} K kg^{-1} and the box is the region of key interest.

5.1 *Distribution of 200-hPa MPV*

At upper levels, MPV2<<MVP1, MPV≈MPV1. Therefore, examining the variation of MPV can clearly reveal the role of MPV1 during the generation and development of the heavy rain. The distribution of 200-hPa MPV can be used to indicate the evolution of disturbances near the tropospause.

In the early stage of the intense rain, the distribution of 200-hPa MPV at 0500 BST June 13 (figure omitted) showed that there were two enclosed centers with a value of 0.3 PVU (1 PVU=10^{-6} m^2 s^{-1} K kg^{-1}, the same below). They were 200 km long in the north-south direction with the central maximum at 0.45 PVU. The two positive areas maintained where they were for several hours. At 1000 BST June 13 (Fig. 2a), the high-value 200-hPa MPV1 disturbances, located in both the northwest and southwest directions, were strengthening and moving toward the east until merging over the delta to form a high-value center, which was corresponding to Stage One of the intense rain. Another positive area, in the southeast-northwest direction, was moving southeastward with a northwesterly airflow and out of the delta at 1400 BST June 13. At that time, a northwesterly flow was at the east side of the delta and a southeasterly flow at the west side, forming an anti-cyclonic circulation over the delta. At the north side of the delta, a north-south-oriented, narrow positive MPV stripe, with a center value of more than 0.6 PVU, was moving toward the southeast to affect the delta once again. At 1500 BST June 13 (figure omitted), the MPV got further strengthened over the delta with the intensity as high as 0.9 PVU, enabling the severe rain to sustain. At 1900 BST June 13, the value of MPV dropped slightly over the delta and rain weakened over most of the area (e.g. Guangzhou and Dongguang). At 2200 BST June 13 (figure omitted), the delta was, once again, affected by positive MPV

values that were on the scales from 10 to 50 km. At the time, a large-scale positive MPV area associated with the disturbances on the westerlies was located northward with the bulk moving to the northeast. Small-scale positive anomalous areas split from the bottom of the trough to affect the delta and the eastern part of the province, signifying the beginning of Stage Two.

5.2 *Distribution of 850-hPa MPV*

In the early stage of the intense rain (0200 BST June 13, 2008, figure omitted), there was a north-south-aligned negative MPV area in the western part of the province. The direction of its long axis is consistent with that of the airflow. For the whole region, the intensity was below -0.3 PVU with an intense center near the shear in western Guangdong. To the south of the shear, there were a number of centers that were below -0.5 PVU. In the few hours that followed, the negative MPV area gradually moved eastward. At 1000 BST June 13 (Fig. 2b), a negative MPV area of smaller than -0.3 was more than 600 km long at the Pearl River Delta through the South China Sea and its long axis remained in the northeast-southwest direction, consistent with that of the airflow. Because of it, the MPV stayed negative for long duration over the delta, i.e., the low-level atmosphere was convectively unstable, resulting in the appearance of Stage One of the precipitation. During the intense rain, the distribution of the negative MPV1 area was very similar to that of the negative MPV area (Fig. 2c). It was moving toward the northeast to affect the delta to make it convectively unstable over an extended period. In comparison, the distribution of low-level MPV1 was well corresponding to that of the upper-level MPV1 in that the heavy rain occurred where the upper-level high MPV1 was allocated with lower-level low MPV1. Disturbances from low-level low MPV1 was the immediate cause for the convective instability.

The distribution of MPV2 was entirely different from that of MPV. In the early stage of the intense rain (0200 BST June 13, figure omitted), MPV2 was positive over a large region in coastal southwestern Guangdong. During the rain, the delta's MPV2 was decreasing while its MPV and MPV1 were increasing. At 1000 BST June 13 (Fig. 2d), MPV2 was positive over a narrow stripe from the eastern delta to the South China Sea, with its long axis oriented in a direction consistent with the airflow. The delta's MPV2 was thus able to maintain positive for extended duration. At 1400 BST June 13, a positive area that was still as long as 600 km over the delta and South China Sea gradually moved to the northeast. At 2200 BST June 13, a fine-scale, positive MPV2 area once again moved from southwest to northeast to affect the delta. It shows that during the heavy rain, the delta's low-level southerly airflow was strong and its warm and humid airflow was active and highly baroclinic.

5.3 *Decomposition of MPV2*

Along 22.8° N, MPV2 was decomposed latitudinally into two terms, $g\left(\frac{\partial v}{\partial p}\frac{\partial \theta_e}{\partial x}\right)$ and $g\left(-\frac{\partial u}{\partial p}\frac{\partial \theta_e}{\partial y}\right)$, for study (Fig. 3). During the daytime of June 13, $g\left(\frac{\partial v}{\partial p}\frac{\partial \theta_e}{\partial x}\right)$ was mainly positive within the range of x=50–80 and below the level of 800 hPa, while $g\left(-\frac{\partial u}{\partial p}\frac{\partial \theta_e}{\partial y}\right)$ was negative most of the time, suggesting that the low-level MPV2 remains positive mainly because of $g\left(\frac{\partial v}{\partial p}\frac{\partial \theta_e}{\partial x}\right)$. At 1600 BST June 13, the cross section of $g\left(-\frac{\partial u}{\partial p}\frac{\partial \theta_e}{\partial y}\right)$ (Fig. 3b) showed a β-scale positive area below 800 hPa at x=70, which is corresponding to the peak of the rain.

Figure 4 gives the temporal curves of latitudinal and longitudinal winds on the levels of 850 hPa, 900 hPa, 950 hPa, and 975 hPa in association with x=60 in Fig. 3. As it shows, the diurnal wind field of June 13 experienced dramatic changes, with larger magnitude with the longitudinal wind than with the latitudinal one. From 0800 June 13 to 0200 June 14, the 850-hPa longitudinal wind underwent a process in which it "descended, ascened, descended, ascened, and descended again" and the 900-hPa longitudinal wind was close to the 850-hPa one in the variation during this period, while the variation of the longitudinal winds at 950 hPa and 975 hPa was much different from that of 850 hPa, thus causing the change in $\frac{\partial v}{\partial p}$ between 850 hPa and 975 hPa. At 1400 to 1600 BST June 13, the v component increased more at 950 hPa than at 850 hPa and $\frac{\partial v}{\partial p}$ increased. If $\frac{\partial \theta_e}{\partial x}$ remains unchanged, $g\left(\frac{\partial v}{\partial p}\frac{\partial \theta_e}{\partial x}\right)$ increased and MPV2 increased. As shown in the variation of the latitudinal wind, the u component increased faster at 850 hPa and 900 hPa than at 950 hPa and 975 hPa during this period of time. At 975 hPa, the previous westerly wind (positive) turned into easterly wind (negative) and turned back to westerly wind again after 2000 BST, suggesting that a 975-hPa mesoscale system was affecting the delta from 1400 to 2000 BST. When $\frac{\partial u}{\partial p}$ decreases between 850 hPa and 975 hPa, and

$g\left(-\frac{\partial u}{\partial p}\frac{\partial \theta_e}{\partial y}\right)$ increases and MPV2 increases if $\frac{\partial \theta_e}{\partial y}$ remains unchanged. Likewise, on the east and north sides of the low θ_e center, $\frac{\partial \theta_e}{\partial x}$ and $\frac{\partial \theta_e}{\partial y}$ were greater than zero. When the isoline of θ_e changes, MPV2 will also change. It is then clear that the baroclinity associated with high values taken for MPV2 is mainly shown in the vertical shear of the longitudinal wind. The growth of shear is related to the activity of low-level southwest-by-south jet streams.

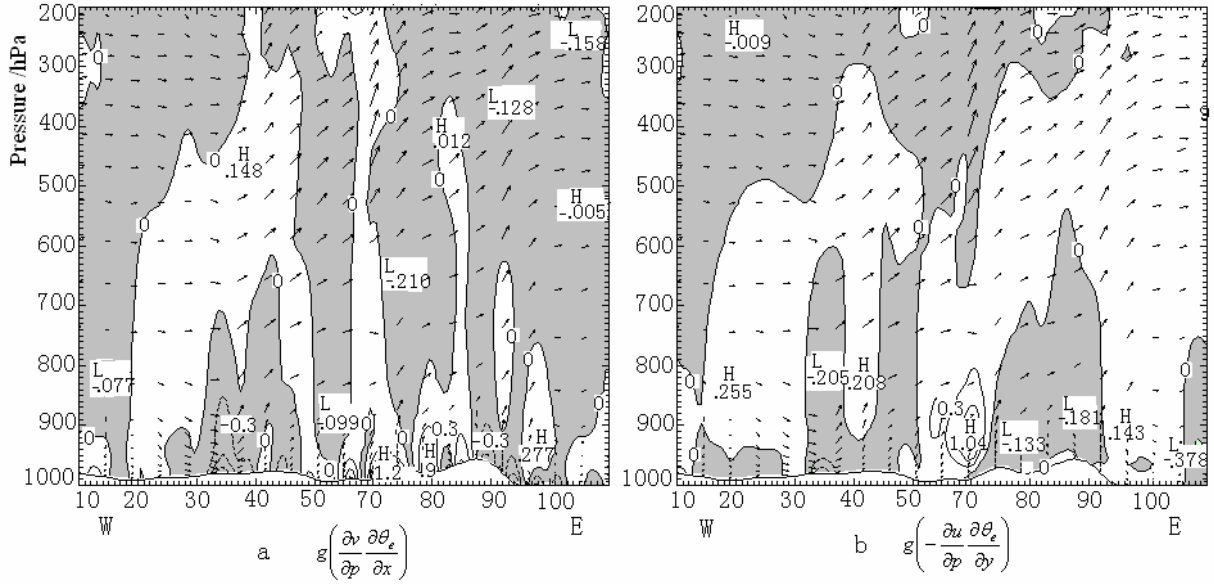

Fig. 3. Vertical cross sections of the heavy rain core simulated for 1600 BST June 13, 2008. The grey areas are for negative values and white areas for positive values.

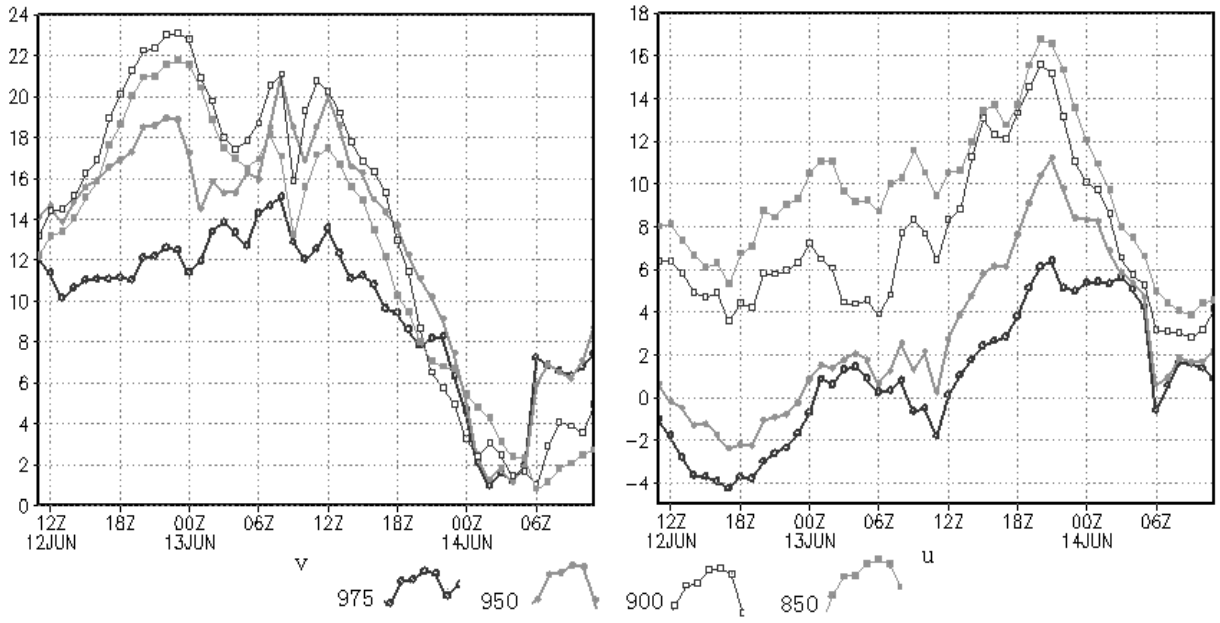

Fig. 4. Curves of temporal variation of the *u* and *v* components at *x*=60 on the levels of 850 hPa, 900 hPa, 950 hPa and 975 hPa as in Fig. 3. Unit: m/s

6 SUMMARY

(1) A rain, the strongest ever during the first yearly flooding season in 2008, took place in Guangdong province from 2000 BST June 12 to 2000 BST June 14. The rainfall center was located over the delta south of the shear. During the intense rain, the low levels of the delta were controlled by southerly airflows south of a shear. The airflows were with such strong convergence of wind speed that unstable energy was transported northward from the estuary of the delta to the delta itself. Under the joint effect of intense upper-level divergence and a 500-hPa westerly trough moving from west to east, a

warm-sector rain occurred over the delta.

(2) Usually, heavy rains take place where high MPV1 at the upper levels is allocated with low MPV1 and high MPV2 at the lower levels. For the rain of interest, the disturbances of the upper-level high MPV1 come from the northwest and southwest while those of the lower-level low MPV1 come from the southwest and those of the lower-level high MPV2 from the south. The disturbances of the lower-level low MPV1 are the immediate cause for convective instability. The allocation of MPV accounts for the activity of warm and humid airflow, high baroclinity, and release of unstable energy, which act to produce intense warm-sector precipitation.

(3) As shown in analysis that decomposes MPV2, changes in the vertical shear of the longitudinal and latitudinal winds drive $g\left(\frac{\partial v}{\partial p}\frac{\partial \theta_e}{\partial x}\right)$ and $g\left(-\frac{\partial u}{\partial p}\frac{\partial \theta_e}{\partial y}\right)$ to change. For the intense rain of interest, the contribution that keeps MPV2 positive below 800 hPa is mainly from $g\left(\frac{\partial v}{\partial p}\frac{\partial \theta_e}{\partial x}\right)$. When the vertical shear of the longitudinal wind increases below 800 hPa, $g\left(\frac{\partial v}{\partial p}\frac{\partial \theta_e}{\partial x}\right)$ increases. When the low level of 975 hPa is affected by mesoscale systems, $g\left(-\frac{\partial u}{\partial p}\frac{\partial \theta_e}{\partial y}\right)$ has explosive growth. It is then understood that the baroclinity with high MPV2 is mainly shown in the vertical shear of the longitudinal wind, and the increase of the shear is related to the activity of low-level southwest-by-south jet streams.

(4) Being a physical quantity that integrates dynamics and thermodynamics, MPV effectively reveals the process of this warm-sector rain in terms of its generation and development and is thus indicative in forecasting the area where the heavy rain would occur.

REFERENCES:

[1] LI Ying, CHEN Lian-shou, LEI Xiao-tu. Moisture potential vorticity analysis on the extratropical transition processes of Winnie (1997) and Bilis (2000) [J]. J. Trop. Meteor., 2005, 21(2): 142-152.

[2] ZHAO Yu, WU Zeng-mao, LIU Shi-jun, et al. Potential vorticity analysis of an torrential rain triggred by a neutercane in Shandong province [J]. J. Trop. Meteor., 2005, 21(1): 33-43.

[3] LAI Shao-jun, HE Fen, ZHAO Ru-ting, et al. The diagnostic analysis of “Longwang” typhoon [J]. Sci. Meteor. Sinica, 2007, 27(3): 266-271.

[4] WU Guo-xiong, CAI Ya-ping, TANG Xiao-jing. Moist potential vorticity and slantwise vorticity development [J]. Acta Meteor. Sinica, 1995, 53(4): 387-398.

[5] ZHANG Duan-yu, DING Zhi-ying, ZHANG Xing-qiang, et al. Relationship between MPV and Meiyu rainstorms in 2003 in Jianghuai area [J]. J. Nanjing Inst. Meteor., 2006, 29(4): 526-532.

[6] WANG Yi-ping, LU Wei-song, PAN Yi-nong, et al. Numerical simulation of a torrential rain in the northeast of Huaihe basin part II: Instability conditions and the mechanism of intensification and maintenance [J]. Acta Meteor. Sinica, 2008(2): 177-188.

[7] REN Yu-long, SHOU Shao-wen, LI Yao-hui. Numerical simulation and moist potential vorticity diagnostic analyses of a heavy rain process in eastern part of Northwest China [J]. Plateau Meteor., 2007, 26(2): 344-352.

[8] FAN Ke, JU Jian-hua. Application of potential vorticity diagnoses in Yunnan summer heavy rain forecasting [J]. Plateau Meteor., 2004, 23(3): 387-392.

[9] MENG Wei-guang, WANG An-yu, LI Jiang-nan, et al. Moist potential vorticity analysis of the heavy rainfall and mesoscale convective systems in South China [J]. Chin. J. Atmos. Sci., 2004, 28(3): 330-341.

[10] WEN Li-juan, CHENG Lin-sheng, ZUO Hong-chao, et al. “98.5” diagnostic analysis of moist potential vorticity anomaly during the May 1998 heavy rainfall of South China in the flood season [J]. J. Trop. Meteor., 2006, 22(5): 447-453.

[11] XIA Ru-di, ZHAO Si-xiong, SUN Jian-hua. A study of circumstances of meso-β-scale systems of strong heavy rainfall in warm sector ahead of fronts in South China [J]. Chin. J. Atmos. Sci., 2006, 30(5): 989-1008.

[12] JEREMY S G, WILLAM A G Jr., STEVEN E K et al. The use of a modified Ebert–McBride technique to evaluate mesoscale model QPF as a function of convective system morphology during IHOP 2002 [J]. Wea. and Forecasting, 2006, 21(3): 288-306.

Citation: LI Jiang-nan, YE Ai-fen, XU Yong-hui et al. Evolution of moist potential vorticity during a warm-zone heavy rainfall event in the Pearl River Delta. *J. Trop. Meteor.*, 2011, 17(3): 310-316.